



UKAEA

Report



# THE INFLUENCE OF A HELICAL FIELD ON A REVERSE FIELD PINCH

D. C. ROBINSON  
T. N. TODD

CULHAM LABORATORY  
Abingdon Oxfordshire

1982



© - UNITED KINGDOM ATOMIC ENERGY AUTHORITY - 1982

Enquiries about copyright and reproduction should be addressed to the Librarian, UKAEA, Culham Laboratory, Abingdon, Oxon. OX14 3DB, England.

# THE INFLUENCE OF A HELICAL FIELD ON A REVERSE FIELD PINCH

D C Robinson and T N Todd

technical support: L J Barrow, S Blewett, B W Foster, B J Parham,  
P J Shatford, R W Storey

(part time  
scientific support): P G Carolan, J J Ellis\*, I H Hutchinson, D J Lees,  
M A Protheroe<sup>+</sup>

Culham Laboratory, Abingdon, Oxon OX14 3DB, UK  
(Euratom/UKAEA Fusion Association)

\*University of Oxford

<sup>+</sup>Royal Holloway College, University of London

## ABSTRACT

The CLEO device has been used to investigate the production of helically stabilised pinch configurations. The slow start-up of a pinch and the influence of a helical field on self reversal, stability and confinement have been investigated. Reverse field pinch and OHTE configurations have been established with plasma currents of up to 85 kA and densities of up to  $10^{14}\text{cm}^{-3}$ . The confinement was found to be degraded by the addition of helical fields. A comparison with other toroidal configurations has been made.

December 1981  
cms





## INTRODUCTION

In the OHTE concept, a new approach to fusion invented by T Ohkawa<sup>[1]</sup>, the pitch reversal necessary in a reversed field pinch (RFP) is assisted by the pitch associated with the helical windings. This permits quasi-continuous operation of an RFP without requiring the regenerative motions (and associated losses) which are usually necessary. CHTE is Japanese for check, as in chess, and is also an acronym for ohmically heated toroidal experiment.

The chief advantages of OHTE over other confinement devices are

- (i) a small reactor design, because the current density in the plasma is not limited by the magnetic field strength of the external coils,
- (ii) ignition is possible by ohmic heating alone because of the high current density,
- (iii) the small size permits a recyclable reactor core permitting a higher wall loading.

These advantages are also features of the reverse field pinch.

The radial variation of the pitch of the magnetic field plays a crucial role in achieving stability to magnetohydrodynamic perturbations in toroidal confinement systems. It is essential to avoid the appearance of minima in the profile of pitch versus distance from the magnetic axis. In a tokamak the pitch increases continuously with distance from the magnetic axis but in devices with a high current (relative to the toroidal magnetic field) avoidance of a pitch minimum requires that the pitch must change sign between the magnetic axis and the plasma boundary. This can be achieved by reversing the sign of the axial (toroidal) field, which is the basis of the RFP. In reverse field pinch devices the reversal is created by plasma turbulence associated with instabilities, which leads to a relaxed reverse field state. One drawback with the RFP concept is that the reversed axial field will decay due to plasma resistivity. It seems that plasma turbulence continuously regenerates the reversal but the losses associated with the turbulence appear to be unacceptable.

In OHTE the pitch reversal can be achieved and sustained by currents flowing in external helical conductors similar to those used in stellarators.



This permits a significant degree of control over the pitch profile independently of the plasma current and potentially extends the duration of the usually transient RFP configuration.

Control of the pitch profile may be achieved by a helical field of any  $\ell$  number. An  $\ell = 3$  field produces acceptably small distortion of the magnetic surfaces and thereby permits the plasma current to flow in relatively close proximity to a conducting wall, so assisting the wall stabilisation of potential instabilities. An  $\ell = 2$  field achieves a similar pitch reversal and requires less power in the helical windings but it produces a greater distortion of the plasma and leaves the plasma further from the conducting wall. Helical equilibrium calculations show that the pitch reversal region associated with the  $\ell = 3$  fields, which lies just inside the separatrix, is very small, typically less than 10% of the plasma radius. The radial variation of the pitch in such a case is very much steeper (as  $r^8$ , as indicated in Fig.1) than for known stable RFP equilibria. These calculations show that the pitch angle of the windings must be in the region of 30-45°. The actual value of the imposed pitch is not very sensitive to the precise angle.

Of particular importance to the OHTE concept, and indeed for most magnetic confinement approaches, is the integrity of the magnetic surfaces in the presence of error fields. The separatrix, which is a feature of most OHTE configurations, is particularly vulnerable to such error fields. Calculations show that the average pitch produced by the helical fields is strongly decreased by the addition of vertical fields or local vertical field errors. Magnetic surface calculations in toroidal geometry also show that the region of pitch reversal is easily destroyed by small error fields. A further effect which can erode the region of pitch reversal is the presence of instabilities in the plasma which produce helical fields and which have an effect on the magnetic surfaces close to the separatrix.

The stability of the OHTE configuration is very similar to that of the ordinary cylindrical reverse field pinch. Pinch configurations do exist which are completely stable to all kinks and tearing modes with zero current at the edge of the plasma. Calculations on OHTE-like configurations show that the helical winding can significantly enlarge the parameter space for interchange-stable finite beta equilibria with pitch reversal while avoiding axial current reversal. The unfavourable curvature associated with the additional helical field may make the already unstable pressure driven resistive mode rather worse than in the reverse field pinch.

The core of the OHTE pinch should be paramagnetic with current density peaked on axis and with a central low shear region which will be subject to turbulent thermal conduction and convection as in an RFP. The translational transform arising from the helical windings may act as an insulator between the turbulent core and the vessel wall. It can do this with vacuum fields and without the necessity for excessive plasma currents close to the first wall as required in the reverse field pinch. It should make it possible to form a quiescent confinement layer in the outer regions of the plasma.

The most attractive feature of the OHTE configuration is that the pitch profile can be controlled and this permits the reversed pitch to be sustained with vacuum fields at the edge of the plasma. An unfortunate consequence of this form of pitch control however is that plasma start-up is likely to be difficult initially, with strong instabilities associated with the small aperture. The integrity of the magnetic surfaces in the region of pitch reversal is in doubt and so pitch control may be much less efficient than expected.

#### CLEO-OHTE EXPERIMENT

The CLEO device is admirably suited to investigating the start-up and



production problems of the OHTE configuration and for making comparisons with reverse field pinches. This device has previously been operated both as a stellarator and as a tokamak. The major radius of CLEO is 90 cm and the minor radius of the vacuum vessel is 14 cm. The vacuum vessel consists of a 25 mm thick stainless steel shell with two toroidal gaps and no poloidal gap. There is no liner. The helical winding consists of one to ten conductors in each direction with  $q=3/7$  and a minor radius of 17 cm. The vacuum vessel time constant is  $\sim 3.6$  ms to vertical and toroidal fields. This is rather interesting as the time constant is comparable to the plasma pulse length and so permits observation on the change of plasma behaviour when the conducting wall is resistive and toroidal flux is conserved for only relatively short times. Initially the Volts/turn were limited to  $\sim 70$  V because of the insulation properties of the 10 conductor  $\ell$ -winding system. The equilibrium vertical field is provided by a set of vertical field control windings in series with the primary windings on the iron core transformer whose current is controlled by shunting the winding with a variable resistance inductance. The iron core provides a flux swing of  $\sim 700$  mVsecs. Primary turns ratios were between 5 and 12 to 1 for the pinches, with a single turn primary used to provide a reverse pre-heat for effective pre-ionisation. The toroidal field is provided on a timescale of seconds, by a winding consisting of 1536 turns with a maximum field of 4.2 kG. A 24 turn fast toroidal field circuit has also been provided which is wound close on to the vacuum vessel. The maximum loop voltage available, since the 10 conductor helical winding has been modified to a single conductor version and various improvements made to the vertical field circuits, is  $\gtrsim 1.3$  kV.

Unlike other reverse field pinches, the CLEO device possesses a rather precise control of the equilibrium position of the plasma using vertical field programming and strong gas puffing facilities with 4 PV10 piezo electric valves giving an injection rate of up to  $1.2 \times 10^{-3}$  torr/ms corresponding to an electron injection rate of  $9 \times 10^{13}$  per  $\text{cm}^3$  per ms. Titanium gettering

of the internal vacuum vessel surfaces has been used between shots. The vacuum base pressure is between  $10^{-7}$  and  $10^{-8}$  torr with gettering.

CLEO has three features that make it particularly interesting in comparison with other RFP and OHTE devices.

(i) There is no liner between the plasma and the conducting wall.

The conducting shell is the vacuum vessel (with two insulating gaps) and it is therefore possible for the plasma current to flow very close to the conducting wall which may improve the wall stabilisation.

(ii) The shell time constant is only 3.6 ms when compared with many 10's of ms on other devices.

(iii) The pitch angle of the helical windings on CLEO is 30 degrees, compared with 45 degrees on the OHTE device at General Atomic, USA.

#### SLOW START-UP

An initial series of CLEO experiments were performed with slow rates of current rise. This was seen as particularly important in attempting to establish the reverse field pinch configuration in a slow and controlled manner. This is relevant to both the proposed RFX device and to establishing the reverse field pinch configuration in a reactor system on a slow timescale ( $\sim 1$  sec). The features seen to be of particular importance are

- (i) controlled gas feed for the plasma yielding controlled plasma density
- (ii) control of the equilibrium position of the plasma to effect the maximum aperture during this rise and,
- (iii) the availability of a good conducting wall very close to the plasma.

With the loop voltage limited to less than 70 V/turn pinches with



currents of up to  $\sim 8$  kA of 8 ms duration with a toroidal field of 300-350 gauss were obtained. To produce such discharges the operating density had to be carefully controlled. Too low a density resulted in an excessive pump-out associated with instabilities. This pump-out was clearly correlated with bursts of MHD fluctuations associated with the slow transition through rational and fractional values of the safety factor  $q$ . These bursts of instability were accompanied by rapid increases in the loop voltage. Too high a density resulted in radiation cooling and a significant decrease in the conductivity temperature. The best behaviour was obtained with the gas puffing set such as to more than balance the pump-out associated with the instabilities. Careful control of the vertical field was also required as the pulse length was much longer than the shell time constant for these discharges. The current waveform was found to be characterised by steps which are correlated with instabilities as shown in Fig.2. The arrows indicate the values of safety factor  $q$  at 1,  $\frac{1}{2}$ ,  $\frac{1}{3}$  and  $\frac{1}{4}$ . A multicoil probe was inserted into these discharges and showed that the current distribution and the radial variation of the safety factor  $q$  was tokamak-like, with  $q$  increasing with radius to  $\sim \frac{1}{4}$  at the wall at current maximum. From the poloidal, toroidal and radial magnetic field perturbations observed with a magnetic probe, it was possible to deduce that the current steps were associated with helical modes with  $m=1, n=1$ ;  $m=1, n=2$ ;  $m=1, n=3$ ;  $m=1, n=4$  as  $q$  passed through the fractional values 1,  $\frac{1}{2}$ ,  $\frac{1}{3}$  and  $\frac{1}{4}$ . The increase in loop voltage, pauses in the rise in plasma density and the poloidal field oscillations taken from the probe are shown quite clearly in Fig.2. If the gas feed from the gas puffing system did not balance the current rise approximately, the current terminated very abruptly in a timescale of about 10  $\mu$ s.

These current steps are reminiscent of the magic numbers observed on the ZETA device<sup>[2]</sup>. The helical modes apparently saturate and rotate with

frequencies in the region of 5-10 kHz. This frequency is quite close to the electron diamagnetic drift frequency for such a plasma. The measured field perturbations are shown in Fig.3 and are rather similar to those measured by Rusbridge and Lees on the ZETA device<sup>[3]</sup>. The radial structure of these perturbations has been compared with that predicted from resistive MHD initial-value calculations (provided that the measured current distribution and the observed average value of beta (in the region of 30%) is allowed for). Figure 3 shows a comparison of the measured and theoretical field perturbations. From such calculations it is possible to deduce that the driving force for the instability comes from the current gradient at the edge of the plasma. Figure 4 shows an expanded waveform of the radial field oscillations which can exist at the same amplitude for many ms.

The addition of helical field does not influence the form of the instability significantly but it does increase the plasma resistance when the winding current is increased to a point where the separatrix approaches the edge of the vacuum vessel. The current steps and density pauses are observed to be rather longer and the maximum current is reduced. These effects are illustrated clearly in Fig.5. Due to these effects of the helical field and the low loop voltage it was not possible to reach sufficiently high values of the pinch parameter  $\theta$ , with sufficient helical field to produce pitch reversal.

Typical plasma parameters measured under these conditions were: densities of up to  $5 \times 10^{13} \text{ cm}^{-3}$ , average values of beta of about 30%, values of poloidal beta close to unity, energy confinement time  $\lesssim 50 \mu\text{s}$  and mean conductivity temperatures of about 6 eV. Gettering and gas puffing experiments indicated that radiation was not a predominant energy loss process. Later measurements with bolometers supported this indication. The magnetic Reynolds number,  $S = \tau_{\sigma} / \tau_A$  where  $\tau_{\sigma}$  is the field diffusion time and  $\tau_A$  the Alfvén transit time, is  $\gtrsim 10^3$  for these low current plasmas and



is probably high enough for the plasma to exhibit a broad MHD spectrum without being strongly limited by resistive dissipation. With the loop voltage limited to  $\lesssim 70$  V it was not possible to obtain discharges with  $q < 1/4$ . Plasma activity was apparently too strong, producing poor confinement, cool plasma and a high resistivity, . Hence the slow current rise experiments were not successful in producing a reverse field pinch configuration or an OHTE configuration.

The gaps in the vacuum vessel were found to be troublesome in these experiments. The flux appearing across each gap was found to differ by very large amounts. This was thought to be correlated with gross MHD activity leading to asymmetric behaviour in one half of the torus compared with the other and to the production of different plasma potentials between the two halves of the torus. Attempts to overcome these differential fluxes and voltages using resistive tapes across the gaps were made. This was initially to assist the stabilising influence of the shell by permitting image currents to cross the gaps in several places and also to tie the potential of the two portions of the shell together. These tapes however were found to fail in a few dozen shots due to radio frequency arcing. Such effects of course would not have been present with a resistive liner inside the device. These early experiments also established that the additional helical field aggravated the gap problems and often led to the plasma current transferring to high power arcs across the gaps. It was occasionally possible to obtain discharges with the loop current being carried by plasma in one half of the machine and the vacuum vessel in the other half. Clearly strong break up of the plasma in the toroidal direction was taking place.

#### "FAST" START-UP (Conventional Slow Pinch)

Modification to the  $\ell$  windings and improvements to the vertical field coil insulation enabled us to increase the permissible loop voltage to 1.3 kV/turn. The rise time of the plasma current was decreased to  $1 \rightarrow 2$  ms

and the production of pinches with currents of up to 85 kA became possible. It was then found necessary to remove the resistive tapes across the two toroidal gaps because these produced

- (i) significant field errors due to the filamentary currents passing through them,
- (ii) vertical field interaction as a result of significant primary current being due to shell currents (dependent on loop voltage).

The removal of the shorts led to high loop voltage transients particularly when the gas density was low. The high loop-voltage noise was eventually suppressed by adding bank capacitors to the  $B_v$  inner winding, the torus gaps and the helical winding feeders. To achieve and sustain plasma currents in the region of 80 kA for 1-2 ms necessitated the addition of an 8 kV capacitor bank to the primary circuit and the doubling of the capacity of the already enlarged 5 kV bank. The first pinch experiments at high plasma currents indicated that the thick stainless steel vacuum vessel was inadequate for toroidal flux conservation. The flux leakage was cancelled using a fast toroidal field circuit consisting of 24 turns wound on top of the helical conductors, driven by one of the old 500 V OH banks. The principal effect of conserving toroidal flux was to prevent the degradation of the reverse field configuration permitting the sustainment of well reversed pinches, as indicated in Figs.6 and 7. The arrows indicate higher poloidal current ( $I_\theta$ ) in this circuit. The toroidal field at the wall can be sustained, reducing the decay of the measured toroidal field on axis so that sustained configurations could be obtained for a period of 1 to 2 ms. Figure 7 shows a similar sequence but at higher  $\theta$  with the production of a reverse field pinch sustained for up to  $1\frac{1}{2}$  ms.

Experiments with differing initial gas fills and levels of gettering indicated that wall recycling played a dominant role in ungettered discharges



(making them somewhat irreproducible) and could be largely eliminated by gettering between shots. The high impurity influx associated with strong wall recycling in ungettered discharges correctly suggested that significantly better loop resistance and therefore plasma currents would be obtained if heavy gettering was used together with the consequently necessary fast gas puffing. To this end the gas injection system was altered from one PV10 operating at 1 bar as a prefill to four PV10's operating at 2 bar primarily as a steady puff throughout the plasma pulse. It was then also noted that loop resistance increases, which were correlated with residual wall recycling, could be essentially eliminated by heavier gas puffing, perhaps as a result of a mantling effect.

Figure 8(a) shows the current, loop voltage and line of sight density waveforms for a typical ungettered pinch discharge. The arrow here indicates rising/higher initial gas fill. It can be seen that densities approaching  $10^{14} \text{ cm}^{-3}$  can be obtained for these plasma currents. Figure 8(b) shows a similar discharge obtained with a gettered vacuum vessel. The plasma density falls very rapidly to below  $10^{13} \text{ cm}^{-3}$  and the plasma current stops rising after the pump out. Strong gas puffing is necessary in this case to bring the density back to values similar to those shown in Fig. 8(a).

To avoid, the possibly damaging initial loop voltage transient before plasma breakdown, a very effective preionisation system was used. This consisted of a low q tokamak-like discharge,  $\sim 1 \text{ ms}$  long, in the opposite direction to the main pulse, with a density  $\sim 4 \times 10^{12} / \text{cm}^3$  leading to a reduction in the initial loop voltage of the main discharge by a factor  $\sim 2$  or  $3$  to  $\sim 300\text{-}400 \text{ V}$ .

With preionisation, gettering and gas puffing, reproducible discharges of both reverse field pinch type and OHTE-like configuration could be obtained.

Reverse field pinches in CLEO are found to fall somewhat to the right



of the usual F- $\theta$  curves as detailed in Fig.9. The correction for porthole effects is also indicated in Fig.9. The porthole corrections are more complicated than usual and have been derived from extended magnetic profiles (with and without plasma) as shown in Fig.10\*. The high values of theta required to achieve reversal can be partly explained by the high average values of beta obtained in CLEO, and also by the near-vacuum edge obtained on the device. These effects are demonstrated in Table 1 for a model configuration which has been matched to the experimental data. In the sigma model  $\sigma = \underline{j} \cdot \underline{B} / B^2 = \sigma_0 (1 - (r/a)^{EN})^2$ , so that EN=2 corresponds to a relatively peaked current distribution. Figure 11 shows the different field configurations for different values of EN while Fig.12 shows the axial current distributions. The data shown in Fig.9 has a systematic error, because a significant amount of toroidal flux has diffused into the plasma from the finite thickness of the conducting shell. This correction can be  $\gtrsim 10\%$ . Even though the value of  $\theta$  in many of the discharges obtained was  $\gtrsim 2$ , detailed probe measurements in the core of the plasma showed no significant helical distortion of the column and the mean field configuration remained axisymmetric. With a helical configuration the usual diamagnetic drift speed effects yield large oscillatory effects in the on-axis  $B_\phi$  field and zero point of the poloidal field which were not seen.

#### CLEO-OHTE CONFIGURATIONS

When the helical windings are energised, the plasma loop resistance is found to increase and the ohmic heating bank settings have to be raised to maintain the same value of the pinch parameter- $\theta$ , i.e. the plasma current. When the helical winding current reaches about 6.2 kA the ohmic heating banks are at their maximum capacity for 57 kA current in an initial toroidal field of 350 gauss. Operation at a higher toroidal field (which at the same  $\theta$  would require higher plasma currents) is therefore not possible. Figures 13 and 14 shows the current and voltage waveforms for RFP and OHTE

\* The help of M K Bevir is acknowledged.



configurations with  $\theta \sim 2.0$  and a plasma current of about 57 kA. The loop voltage at current peak is significantly higher in the OHTE case than in the RFP.

Although the true OHTE configuration has a separatrix entirely within the vacuum vessel, such operation has been found to be non-optimum by stellarator groups because of the susceptibility of the separatrix to error fields so it was considered that the maximum tested ratio of helical current to plasma current of about  $1/8$  is reasonable for the OHTE configuration. Field line tracing calculations for the CLEO device show that the last closed flux surface touches the inside wall at this ratio (see Fig.26) i.e. the separatrix is on the vacuum vessel wall. Figure 15 shows the measured field configuration at a current of 57 kA for an initial toroidal field of 350 G. The corrections associated with the probe porthole are indicated. Figure 16 shows the equivalent OHTE configuration for the same plasma current and initial bias field. In this case the helical current was 6.2 kA per filament. It can be seen that the OHTE configuration possesses rather less paramagnetism and edge reversal than the reverse field pinch. The axial current distribution is relatively uniform in the core of the plasma and falls to zero at the edge of the plasma. The pressure profiles which can be deduced from these measurements (toroidal effects were neglected because the aspect ratio is  $\sim 7$ ) are shown in Figs. 15 and 16. The values of average beta and poloidal beta are indicated in Table 2.

Table 2 shows detailed comparisons of the parameters associated with reverse field pinch and OHTE configurations for two values of initial bias field, 350 and 500 G. These two comparisons are for configurations with significant field reversal and for configurations where the reversal is  $\sim$  zero. The latter case is thought to be a more precise test of the OHTE configuration, as the contribution to pitch reversal produced by the helical winding should be more significant. As the Table shows, the loop voltage for both scenarios is higher in the OHTE case than in the RFP case. Thus the mean conductivity



temperature is somewhat less in the OHTE configuration than in the reverse field pinch though the mean radius of the OHTE configuration ( $\approx 13\text{cm}$ ) offsets this to some extent. The mean conductivity temperature is  $\sim 35\text{ eV}$  for the reverse field pinch indicating a conductivity temperature on axis of about  $50\text{ eV}$ . The mean density is between  $4$  and  $8 \times 10^{13}\text{ cm}^{-3}$ . The corresponding beta value is about 10% with poloidal beta value  $\sim 0.2 \rightarrow 0.3$ . The energy confinement time is deduced as being between  $10$  and  $20\text{ }\mu\text{s}$  with significantly smaller values for the OHTE configuration.

The best results have been obtained with a reverse field pinch operating at a current  $\sim 85\text{ kA}$  with an initial bias field of  $600\text{ G}$  and a loop voltage of  $\sim 200\text{ V}$ . The OHTE configuration could not be produced at  $85\text{ kA}$  because of the adverse effects of the helical field.

The probe data, which seems to give sensible pressure profiles, leads to values of density and temperature consistent with those obtained from other estimates. Density information has been obtained both with a  $2\text{ mm}$  interferometer and an inserted Langmuir probe, establishing that with gettering and strong gas puffing the density rises towards  $10^{14}\text{ cm}^{-3}$  and is generally sustained at this value until core saturation terminates the plasma current. Figure 17 shows the time variation of the saturation current obtained from the Langmuir probe for a RFP at three different radii.

Bolometer measurements of all these discharges have also been made. These show that the total power loss observed by the bolometer, which is also sensitive to charge exchange losses and was calibrated with a sequence of discharges using neon only, is usually a few tens of per cent of the total input power.

After allowances have been made for the geometry differences between this device and other slow sustained RFP's, the plasma impedance values compare favourably e.g. with ETA/BETA II, ZT-40, HBTXIA and TPE-1RM. The



current density is comparable to that in ZT-40 and HBTXIA but lower than that in ETA-BETA II and TPE-1RM.

In all circumstances when the helical windings have been energised the helical field has

- (i) tended to produce gap breakdown particularly with pulse durations  $> 2$  ms,
- (ii) increased the loop voltage so that the bank settings had to be raised to maintain a given plasma current,
- (iii) lowered the paramagnetism and reduced the tendency towards reversal at the wall,
- (iv) created delays and discontinuities in the plasma current rise as the OHTE configuration was established.

#### COMPARISONS OF VARIOUS TOROIDAL CONFIGURATIONS

CLEO has been used to compare the confinement properties of various toroidal systems, namely tokamaks, a stellarator, a reverse field pinch and an OHTE configuration. This comparison was undertaken at an average magnetic field for the different configurations in the region of 1.8 kG. A comparison could have been made at similar densities but this would have required much larger toroidal fields ( $\sim 10$  kG) for the tokamaks and stellarator. It can be argued on the grounds of Larmor radius effects and classical confinement scaling that comparisons should be made at comparable total magnetic fields.

The comparison was made using electrical diagnostics for  $T_o$ , inter-



ferometric measurements for density, and bolometry for radiation and charge exchange losses. This permits estimates to be made of the average electron temperature, average beta and energy confinement time. These values will necessarily be minimum ones because of the nature of the methods used to make the comparison. Nevertheless it is believed from other more detailed measurements of plasma parameters in similar devices that the differences between the configurations would not be modified by more detailed measurements of the gross plasma parameters. Because of the short shell time constant, programming of the vertical and toroidal fields was necessary to control the plasma position and ensure toroidal flux conservation. Gettering was used throughout and in each case the gas puffing rate was adjusted to produce the maximum attainable density without any obvious transfer to radiation dominated phenomena. All experiments were performed with a 5/1 primary turns ratio.

The different safety factor (or  $q$ ) profiles for the various configurations are shown in Fig.18. The helically assisted low  $q$  tokamak (HALQT) should be noted in that it uses a reverse transform to permit higher values of plasma current, or lower  $q$  and thereby potentially higher values of density and beta. Typical waveforms for the tokamak, HALQT, stellarator, RFP and OHTE modes are shown in Figs. 19, 20, 21, 22 and 23. All of the discharges were optimised for pulse duration by adjusting the ohmic heating, vertical field control system and gas injection systems. The pinch durations were ultimately limited by the 0.7 V sec swing of the iron core. The longest pulses were limited by the vertical field programming error arising from the magnetisation current. The principal results are tabulated in Table 3. The plasma currents range from 1 to 67 kA and the densities from  $2 \times 10^{12} \text{ cm}^{-3}$  to  $8 \times 10^{13} \text{ cm}^{-3}$ . The different maximum attainable densities for these ohmically heated systems are in agreement with the near universal scaling of current to line density ratio,  $I/N = 2.10^{-14} \text{ A.m}$ . This is shown for the different CLEO configurations in Fig.24 by comparison with many other pinch and tokamak devices. It is clear that the different configurations



on CLEO are close to this optimum.

The radius of the RFP configuration is taken as the wall radius, 14 cm, even though there are two limiters of 13 cm radius. This is because at these modest temperatures the limiters are unlikely to be effective for pinches, in which the field lines at the wall spiral principally poloidally. For the tokamaks the limiters are probably effective and the radius is taken as 13 cm. For the stellarator, helically assisted low  $q$  tokamak and OHTE the plasma size is determined by three dimensional field line tracing with the plasma modelled as a single current filament carrying the plasma current, together with an appropriate vertical field to ensure the positional equilibrium of the ring current. Figures 25, 26 and 27, show the shape of the surface of the last closed field line for the stellarator, HALQT and OHTE. The effective aperture radius in each case is  $\sim 9, 10$  and  $13$  cms respectively. The mean conductivity temperature is derived from the measured impedance allowing for the plasma size and assuming  $Z_{\text{eff}}=2$ . In all cases the torus walls are gettered so it is possible that  $Z_{\text{eff}}$  is nearer to 1. For the pinch discharges an additional factor of 4 has been used to correct for the current distribution<sup>[2]</sup> associated with a pinch parameter,  $\theta \sim 2$ . The mean conductivity temperatures vary by only a factor of two for the different configurations. The central temperatures,  $T_0$ , are estimated from temperature distributions measured elsewhere in the different configurations. In no case does the temperature exceed 100 eV. The percentage radiated power is significant and varies from 20-40%. The Table shows the electron poloidal beta, average beta and electron energy confinement time.

The stellarator exhibits the best confinement time but with a small value of beta. This result is borne out by other investigations of stellarator devices. The low  $q$  tokamak is not far behind with a confinement time which corresponds fairly well with that predicted from empirical scaling laws. The



HALQT has a lower confinement time, which appears to be similar to that obtained on other low  $q$  tokamak devices when  $q \lesssim 1.5$ . In this case the current  $q_I$  near the separatrix is in the region of unity. It is possible in this case that the average value of beta is in the region of 1% including the ions since the equipartition time and energy confinement time are similar. Without the helical field the critical beta value for ideal MHD ballooning mode stability is 0.6% for a  $q$  on axis of 1 (Alan Sykes, private comm.). The two pinch configurations produce high average values of beta, possibly up to 6% depending on the ion component, but with rather short energy confinement time,  $< 15\mu s$ . This is a factor 20-40 worse than the other configurations and represents a very severe anomalous loss process. Because the classical confinement time at constant field and temperature scales inversely as the density it might be thought that this could account for the poor confinement of the pinch as it is at a higher density, however the Pfirsch-Schulter correction factors for the other configurations almost cancel this density effect. Thus the neo-classical energy confinement time for the various configurations is almost the same, at  $\sim 1$  ms.

## CONCLUSIONS

The low loop voltage work showed that it was impossible to establish a reversed field pinch with slow current rise. The strong plasma activity was associated with fractional values of  $q$  and led to rapid pump-out.

The production of both sustained reverse field pinch and OHTE configurations was possible with increased loop voltage, in the region of 400 V/turn. Plasma currents up to  $\sim 85$  kA at densities of  $10^{14} \text{ cm}^{-3}$  were obtained. The decay of toroidal flux was compensated by adding a fast toroidal winding and the plasma position was maintained accurately using a controlled vertical field; both of these to compensate for the shell time constants being small compared to the plasma duration.



The gas puffing and gettering experiments showed that it was possible to control the plasma density in such experiments despite the strong pump-out associated with instabilities. With CLEO ungettered it was found that wall recycling could maintain or even increase the electron density during the sustainment phase of the pulse, but when the wall was gettered the electron density peaked rapidly and then decayed to a low value unless substantial gas puffing was employed.

Magnetic probe data shows that the OHTE configuration exhibits less paramagnetism and less reversal for a given theta value than the reverse field pinch. The helical field apparently hinders the self reversal process. From the increased resistance and similar plasma density it can be inferred that the OHTE configuration has poorer energy confinement than the reverse field pinch. In these discharges it is certain that the residual instabilities in the pinch configuration are sufficient to destroy the pitch reversal produced by the helical winding due to ergodic behaviour near the wall.

It is possible that on a larger reverse field pinch device at higher plasma currents, where the MHD activity is reduced that a helical field may lead to some improvement in the confinement of the sustained RFP. Nevertheless the sensitivity of the small region of the pitch reversal to field errors bearing in mind the perturbations produced by internal fluctuations of the pinch, leads to concern over the ultimate potential of this confinement concept.

This series of experiments has established that it is possible to produce a sustained reversed field pinch within a conducting wall which has a time constant less than the pulse duration of the plasma.

A comparison of the confinement properties of different toroidal

configurations, namely the RFP, stellarator and tokamak reveals that the stellarator possesses superior confinement but at low beta while the pinch obtains high beta but with poor confinement. The tokamak confinement is a factor 2 or 3 down on the stellarator depending on the safety factor, but it produces an optimum combination of  $\beta\tau_E$  on this device.

#### REFERENCES

- [1] Ohkawa T, Nuclear Fusion (1980) 20, 1464
- [2] Burton W M et al, Nuclear Fusion, Suppl 1962, Vol.3, 903.
- [3] Lees D J, Rusbridge M G, Saunders P A H, Nuclear Fusion, Suppl. 1962 Vol.3. 895.



TABLE 1

SIGMA MODEL AND  $\theta$  FOR REVERSAL

EN	$\beta(0)$	$\beta_\theta$	$\theta(\text{reversal})$	Remarks
21	0	0	1.27	close to Taylor model
21	5%	0.10	1.35	
21	10%	0.18	1.41	
4	0	0	1.52	
4	5%	0.16	1.67	
4	10%	0.28	1.79	
2	0	0	1.74	
2	5%	0.23	1.99	
2	10%	0.38	2.19	

(Pressure profile not necessarily Suydam stable,  $P=P_0(1-r^4/a^4)^2$ ).

Thus for small  $\beta_\theta$ :  $\theta_{\text{reversal}} \approx \theta_{\text{reversal}}^{(\beta=0)} + \beta_\theta$

TABLE 2

	<u>RFP</u>		<u>OHTE</u>		<u>UNIT</u>
$B_{\phi}$	350	500	350	500	G
$I_p$	57	67	57	67	kA
$I_{hel}$	0	0	6.2	6.9	kA
F	-0.43	$\lesssim 0$	-0.29	$\gtrsim 0$	-
$V_{loop}$	400	$\sim 300$	500	$\sim 400$	V
$\bar{T}_{\sigma}$	18 $\rightarrow$ 25	$\rightarrow 34$	17 $\rightarrow$ 23	$\rightarrow 31$	eV
$\bar{T}_{\sigma-axis}$	36 $\rightarrow$ 45	$\rightarrow 60$	34 $\rightarrow$ 40	$\rightarrow 55$	eV
$\bar{n}_e$	4 $\rightarrow$ 8 x 10 <sup>13</sup> similar		4 $\rightarrow$ 8x10 <sup>13</sup> similar		cm <sup>-3</sup>
$\bar{\beta}$	0.10	$\sim 0.1$	0.12	$\sim 0.1$	-
$\beta_{\theta}$	0.22	$\sim 0.2$	0.20	$\sim 0.2$	-
$\tau_E$	6 $\rightarrow$ 14	<19	5 $\rightarrow$ 10	<17	$\mu s$
$\beta_{\theta}$ probe	0.24	0.17	0.31*	0.27	-
" $\theta$ "	2.0	1.7	2.0	1.7	

\*derived from simple cylindrical pressure balance; with no account of helical fields.



TABLE 3

## CLEO CONFIGURATION COMPARISONS

 $B_\phi = 1.8 \text{ kG, } D_2 \text{ Gas}$ 

	$I_p$ (kA)	$I_L$ (kA)	$R(\text{m}\Omega)$	$\bar{T}_\sigma$ (Z=2, F=4)	$\bar{a}$	$T_o$	radi- ated power %	$\bar{n}_e$ $10^{12} \text{ cm}^{-3}$	$\beta_\theta^e$	$\bar{\beta}_e$ (%)	$\tau_E^e$ ( $\mu\text{s}$ )	$\tau_{\text{pulse}}$ (ms)	$\bar{\beta}_e \tau_E^e (\text{arb})$
RFP	67	0	4.5	20	14	40	$\sim 40^*$	80	0.07	3.1	7	3.5	21.7
OHTE	67	6.9	6	18	13	36	$\sim 40^*$	80	0.07	2.8	5	2.5	14.00
TOK (high q)	4	0	1	23	13	70	37	2	0.49	0.06	209	16	12.5
TOK (low q = 2.5)	6.7	0	0.7	29	13	90	30	5.5	0.60	0.20	372	12	74.4
HALQT (q=1)	11.5	8.5	1	33	10	100	40	17	0.42	0.72	180	15	129.6
Stell	1	11.8	3	18	9	56	16	3.5	5	0.07	760	35	53.2

\*total integrated radiated power through shot.

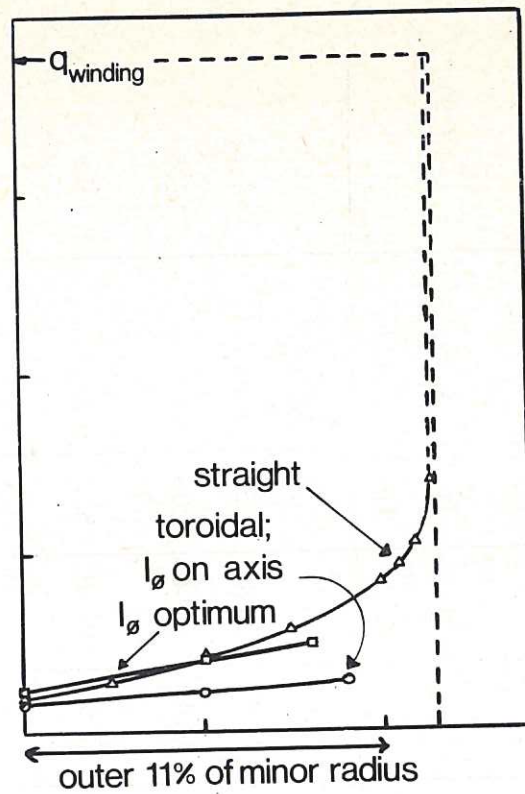


Fig.1 Effect of helical winding fields on purely poloidal field.

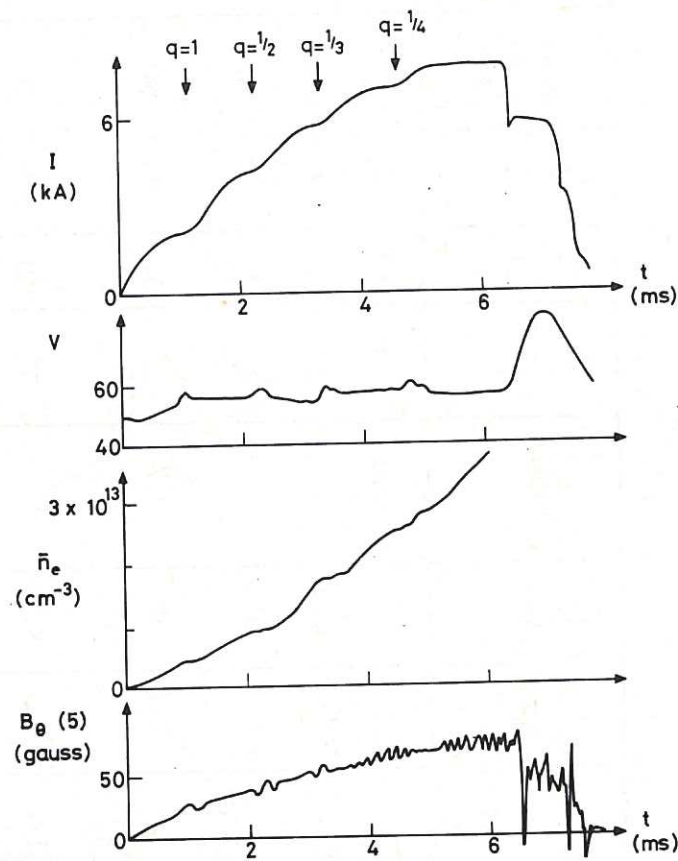


Fig.2 Plasma current, voltage, density and internal poloidal field waveforms.



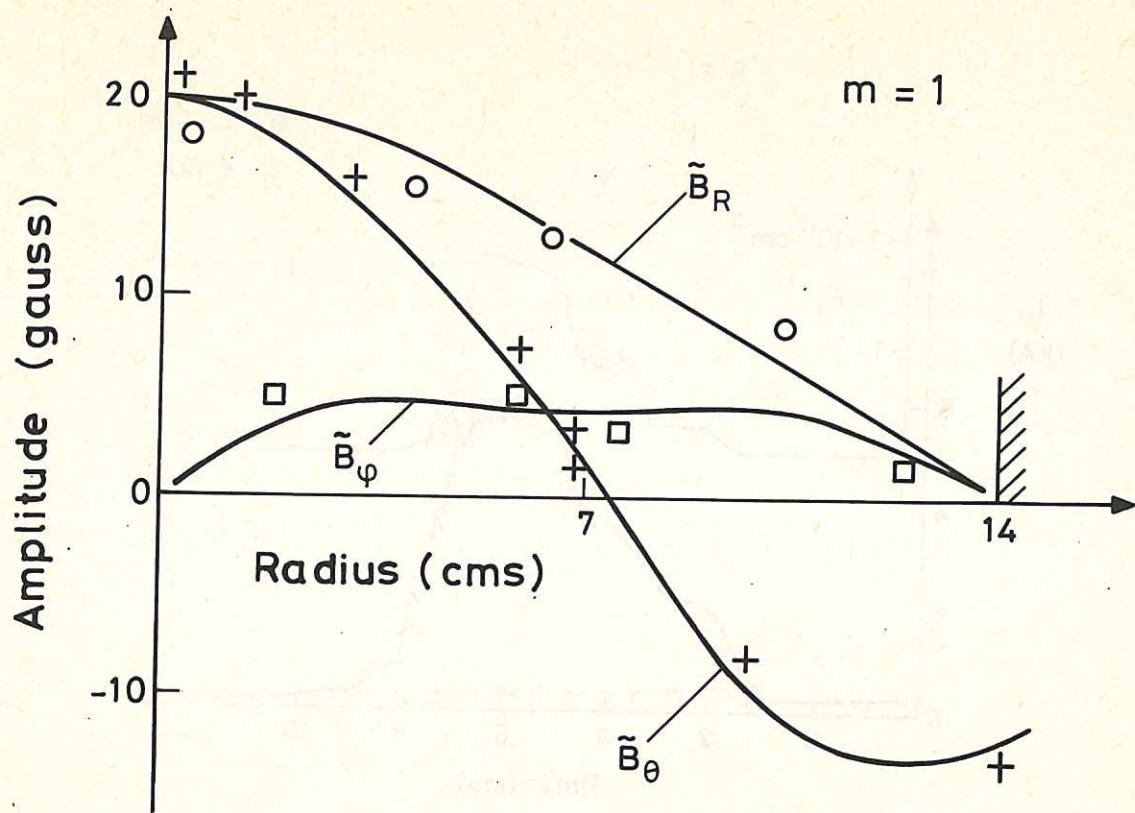


Fig.3 Comparison of measured and theoretical field perturbations.

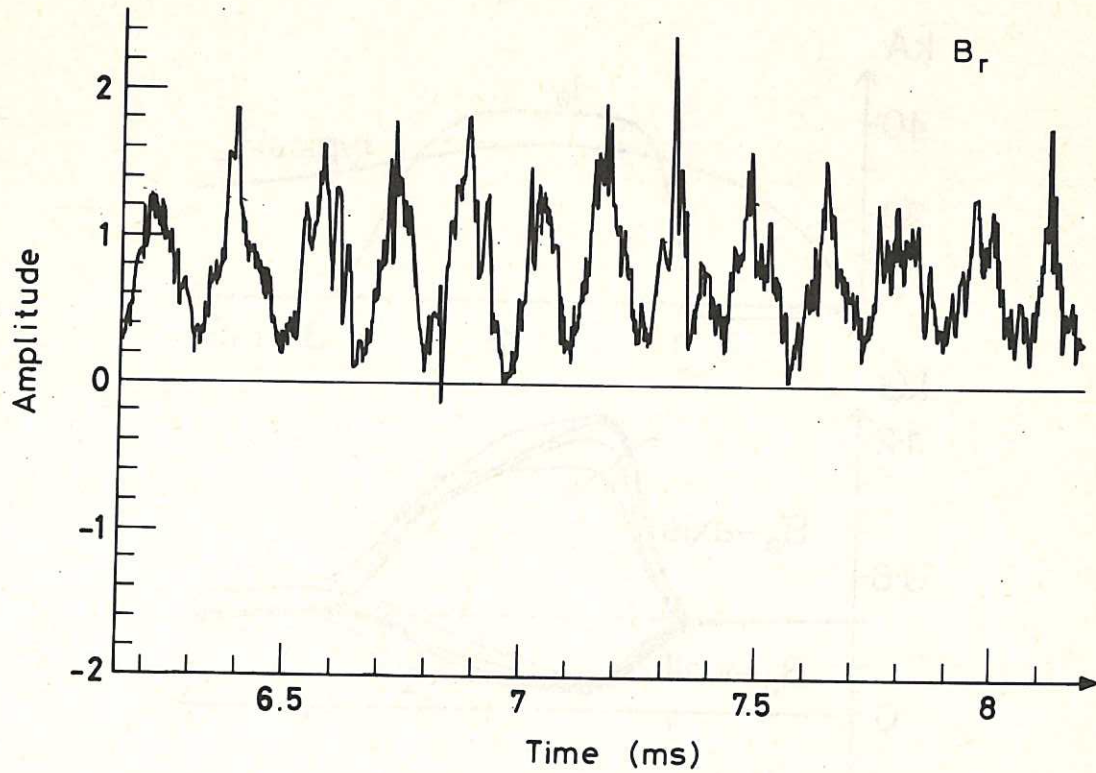


Fig.4 Radial field amplitude as a function of time for a slow start-up pinch.

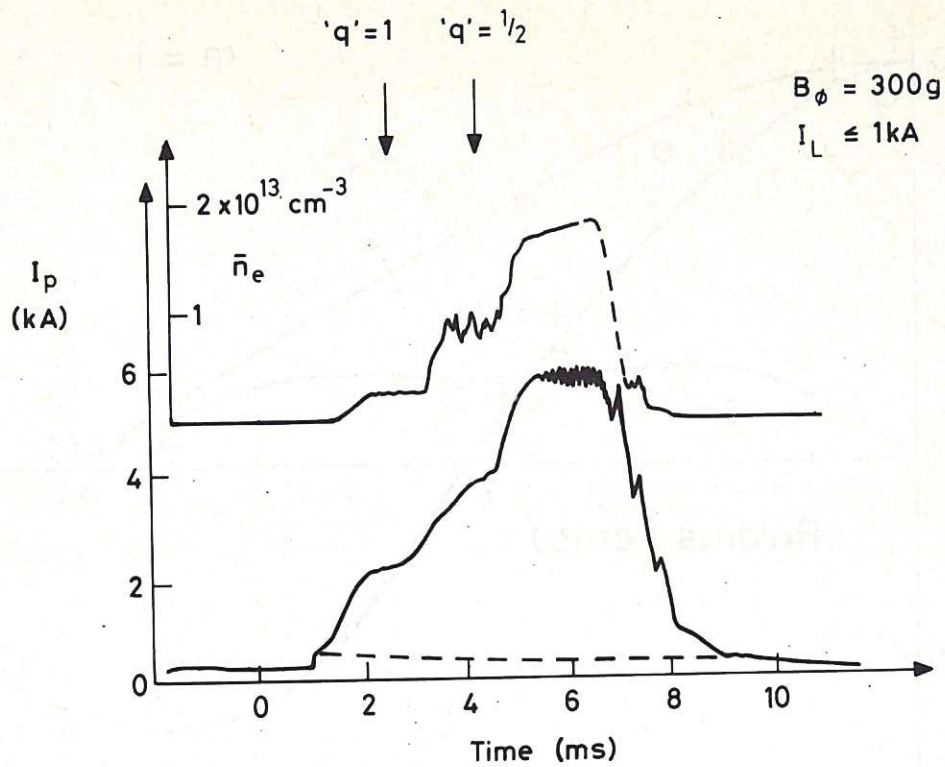


Fig.5 Current steps and density pauses for a slow start-up pinch with a helical field transform opposing the ohmic transform.

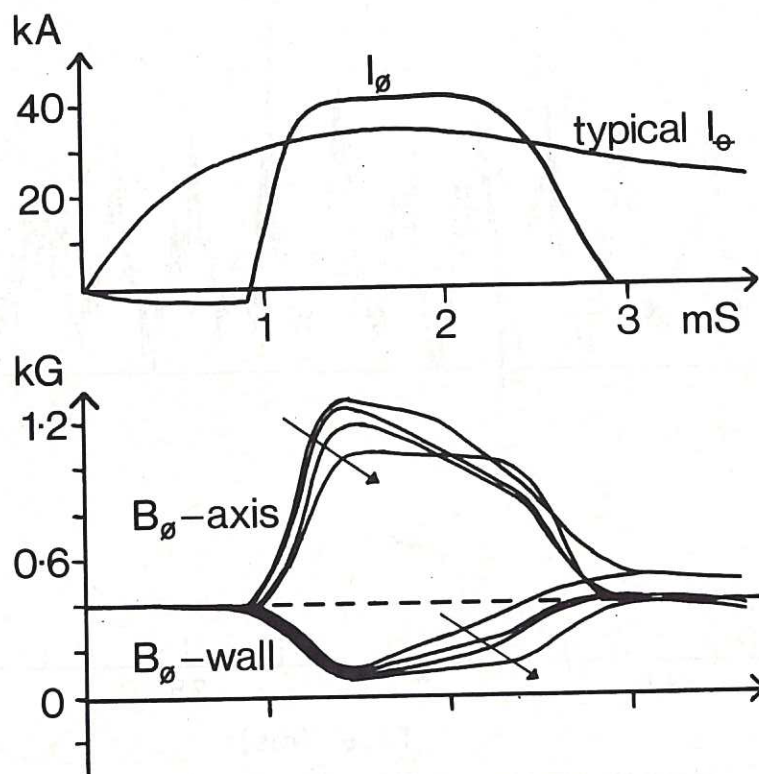


Fig.6 Effects of toroidal field conservation circuit (fast  $B_\phi$ ). Arrows indicate higher  $I_\theta$  in this circuit.



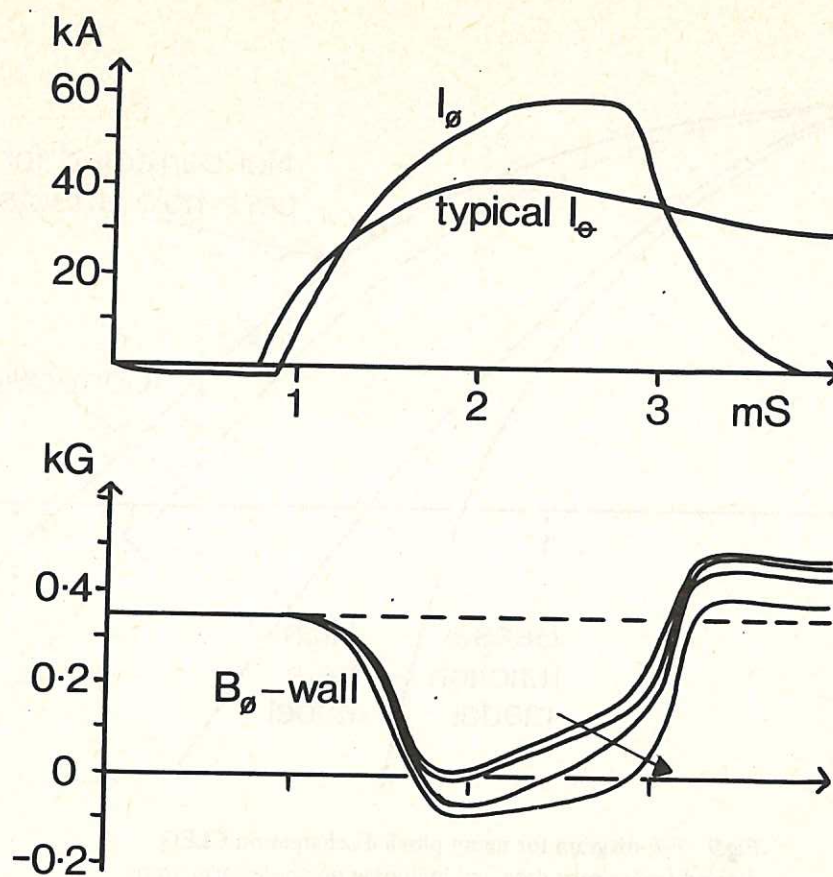


Fig.7 Effect of toroidal field conservation circuit (fast  $B_\phi$ ) on toroidal field at the wall at reversal.

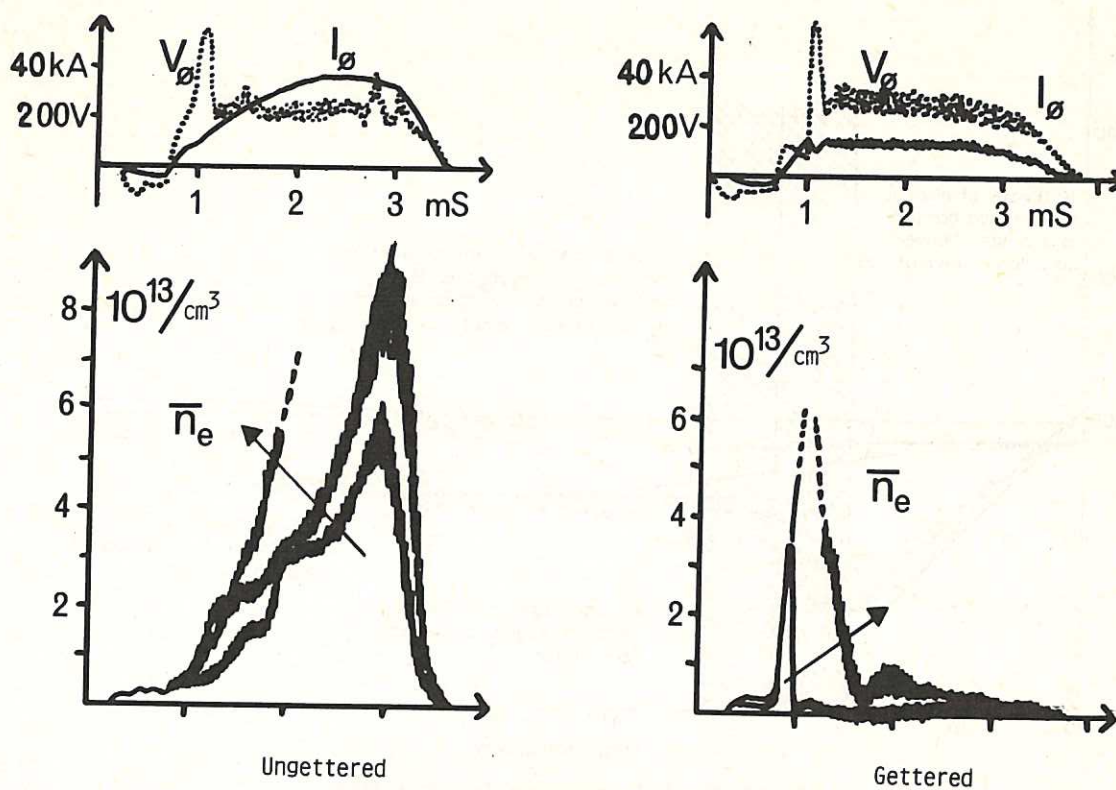


Fig.8 Effects of gettering on wall recycling. Arrows indicate higher initial gas fills, which were similar for both cases.

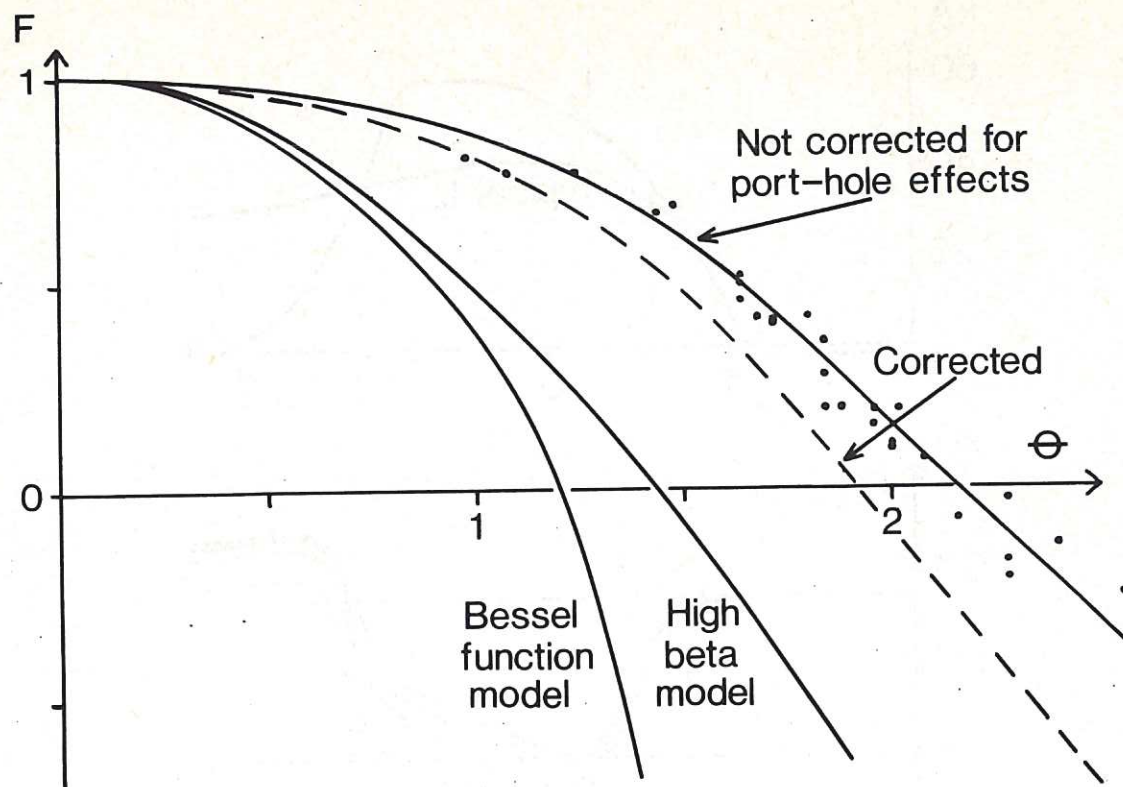


Fig.9  $F-\theta$  diagram for many pinch discharges on CLEO derived from probe data and including porthole corrections.

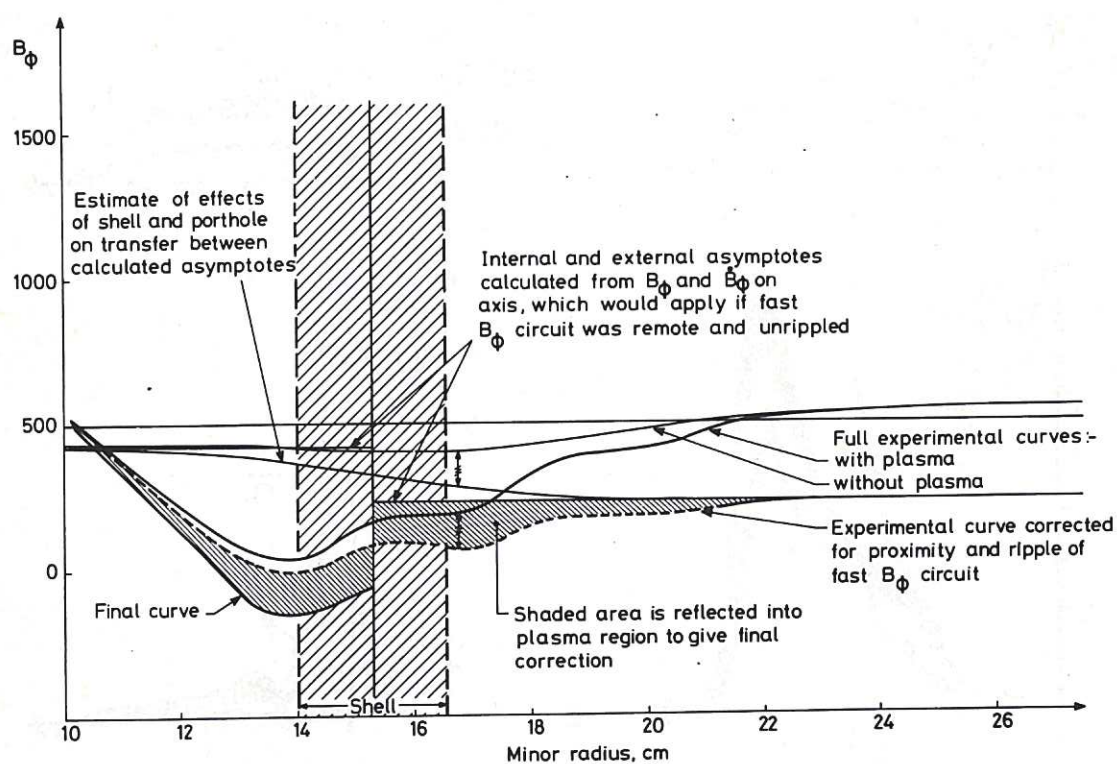


Fig.10 Porthole corrections for 500 G RFP.



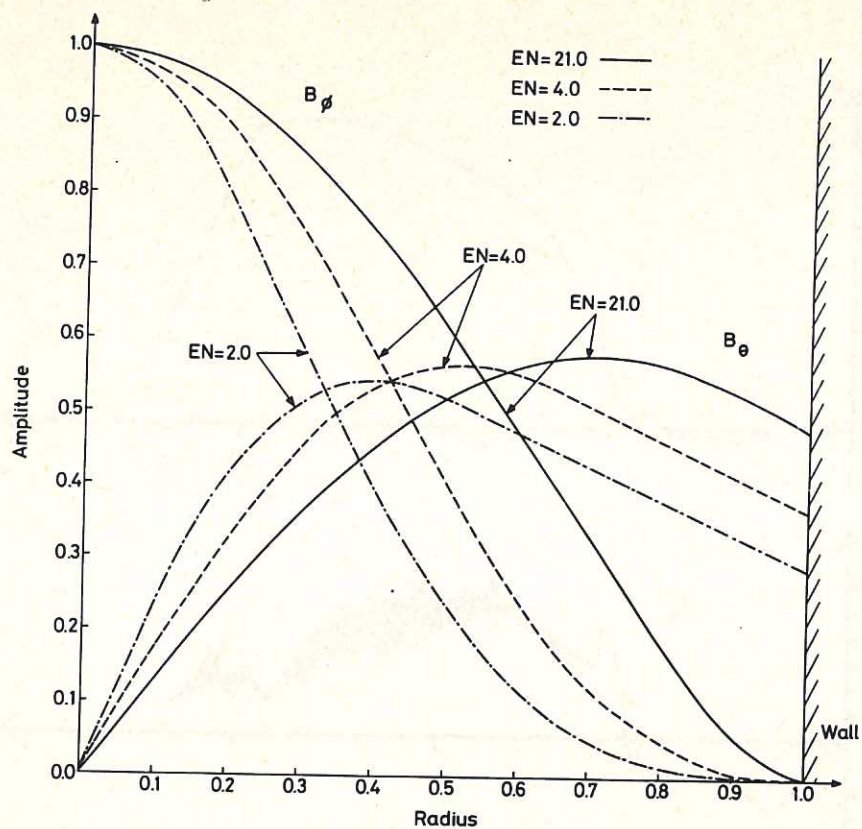


Fig.11 Field configurations for the sigma model with three values of  $EN$  for the toroidal field zero at the wall.

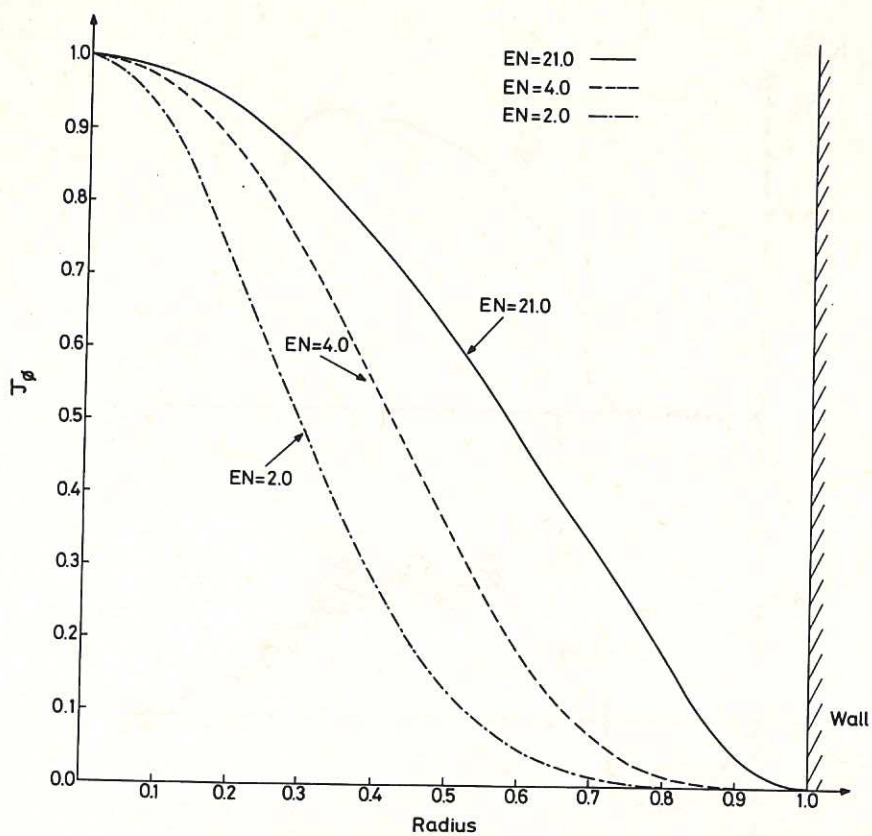


Fig.12 Axial current distributions for the three values of  $EN$ .

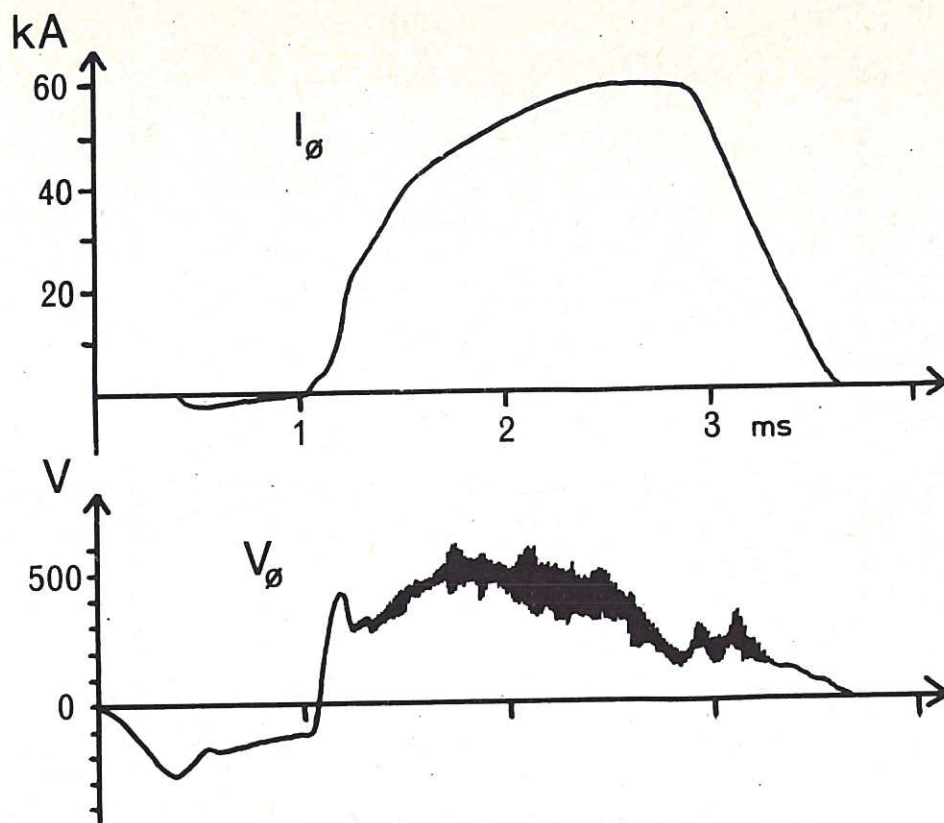


Fig.13 Reversed field pinch current and voltage waveforms for an initial field of 350 G.

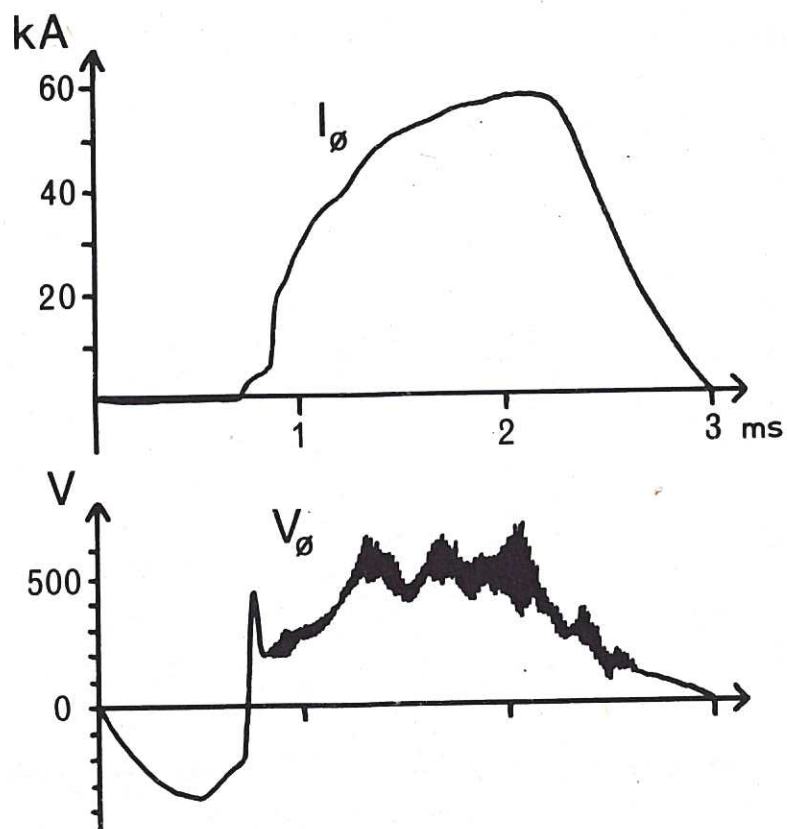


Fig.14 OHTE current and voltage waveforms for an initial field of 350 G.



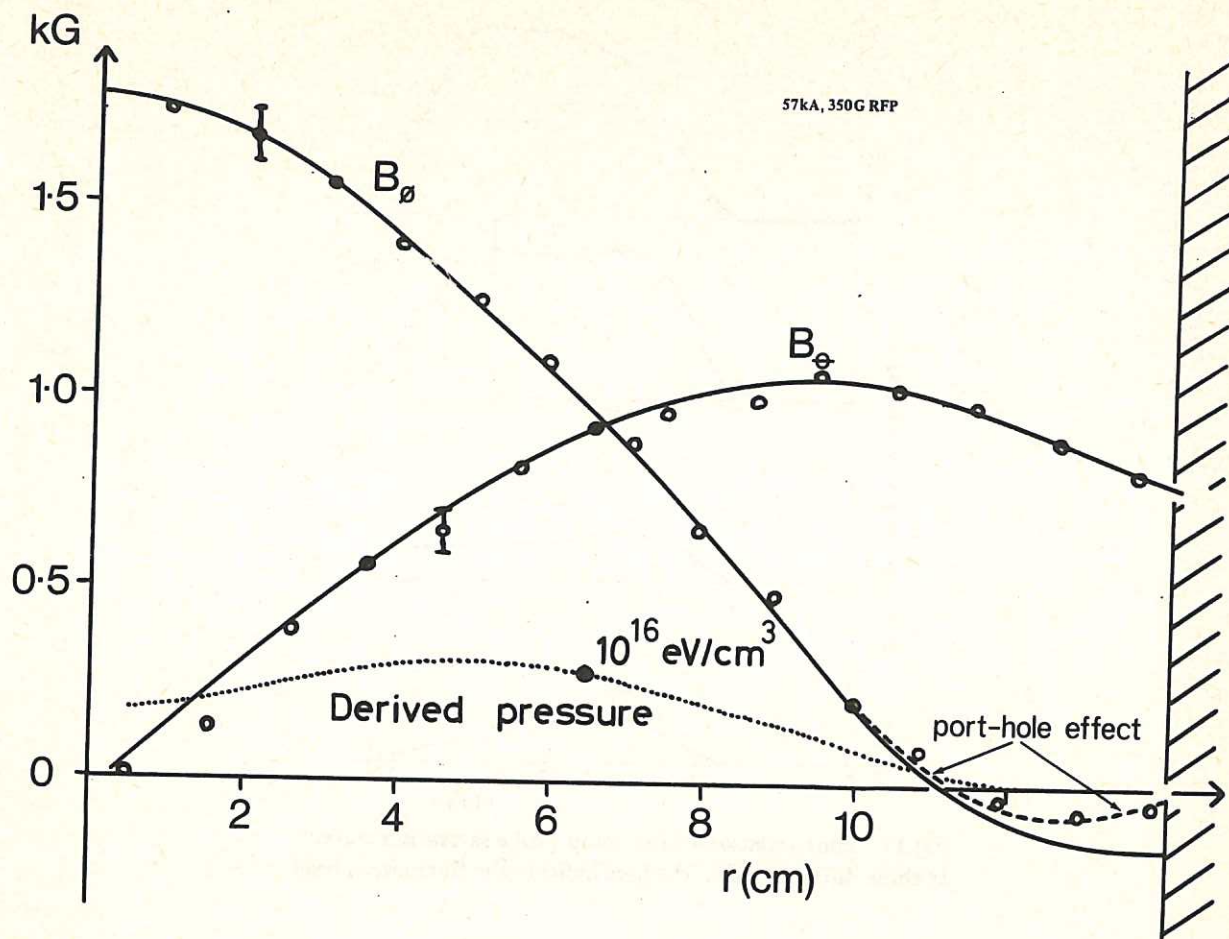


Fig.15 Measured reverse field pinch configuration at 57kA with derived pressure. (Probe approximately vertical).

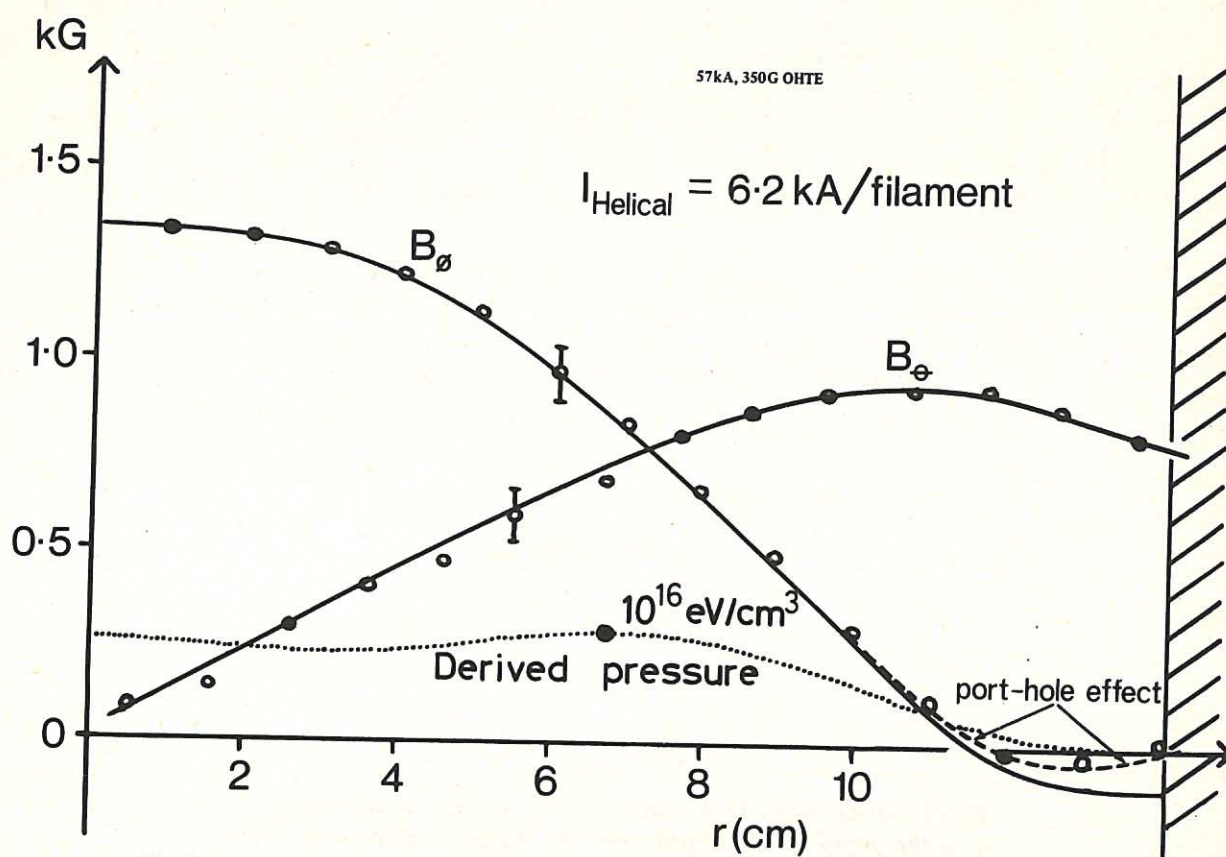


Fig.16 Measured OHTE configuration at 57kA at  $I_{\text{helical}} = 6.2 \text{ kA}$  with derived pressure.

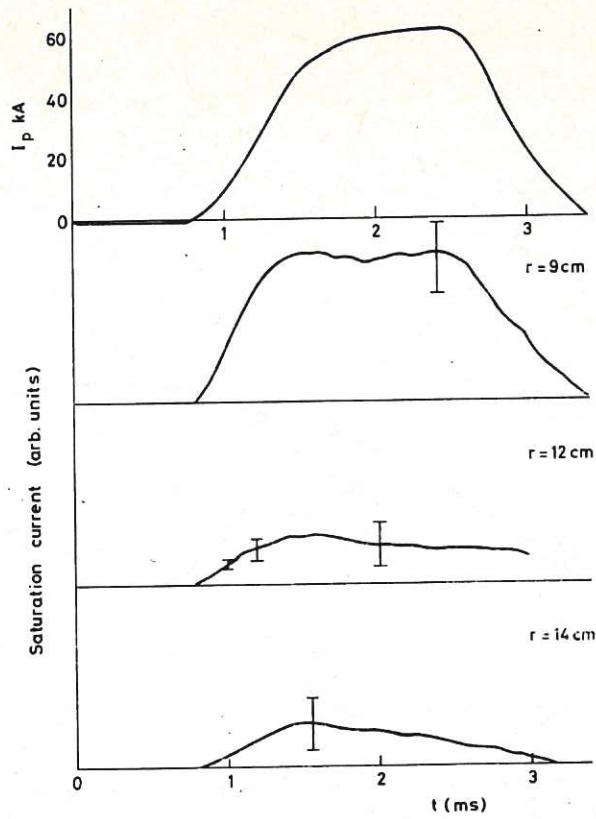


Fig.17 Time variation of Langmuir probe saturation current at three different radii. The bars indicate the fluctuation level.

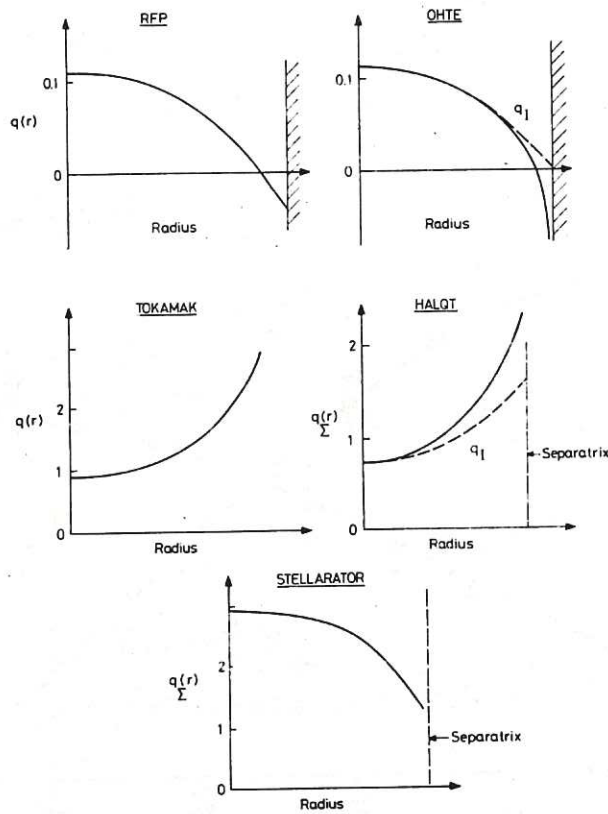


Fig.18 Safety factor or  $q$  profiles for five toroidal configurations.  $q_1$  is the safety factor derived from the current distribution alone.



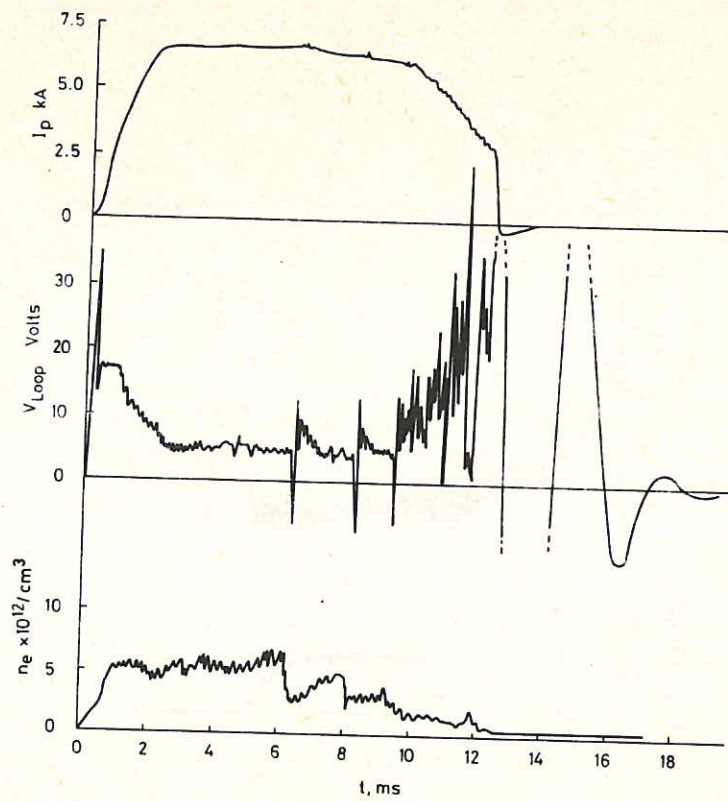


Fig.19(a) Current, voltage and density evolution for a low  $q$  tokamak.

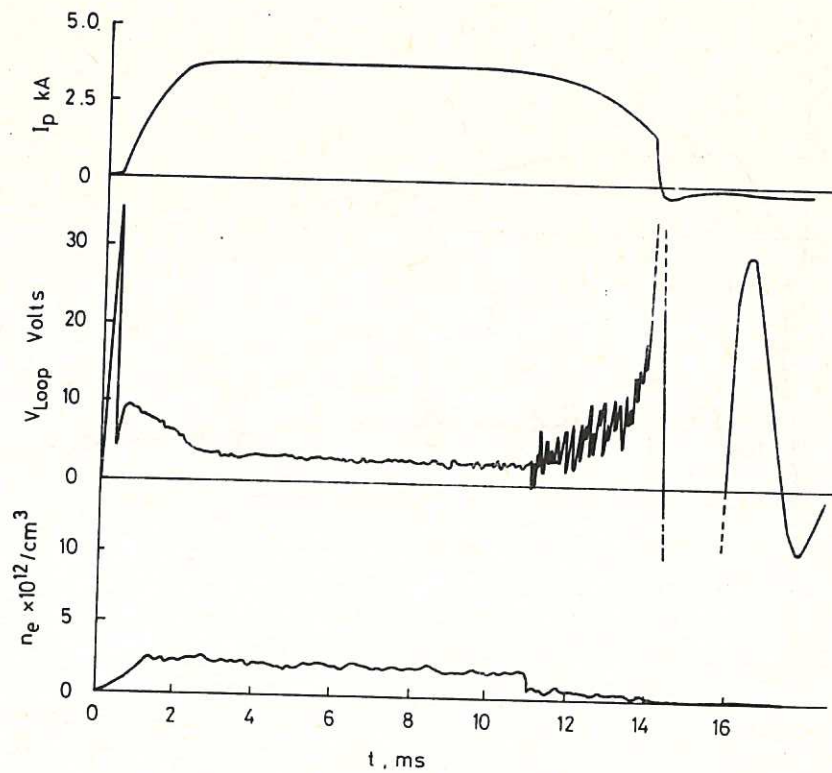
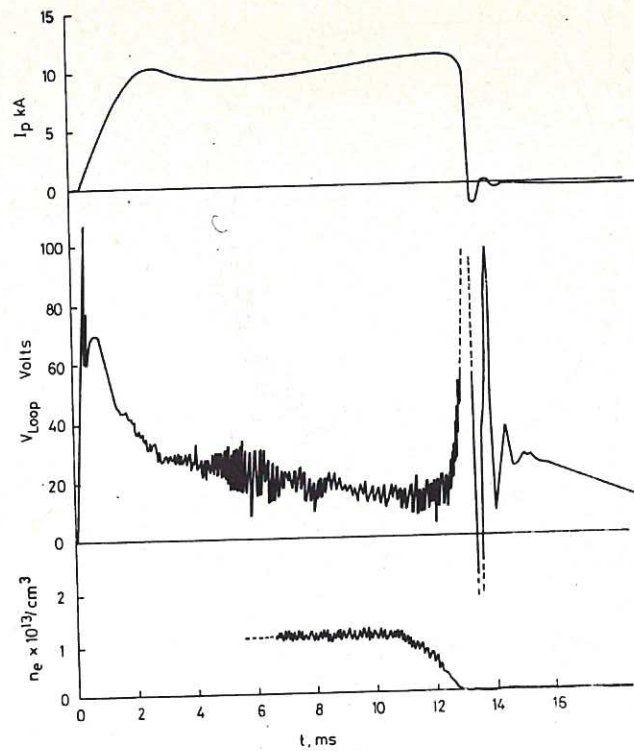
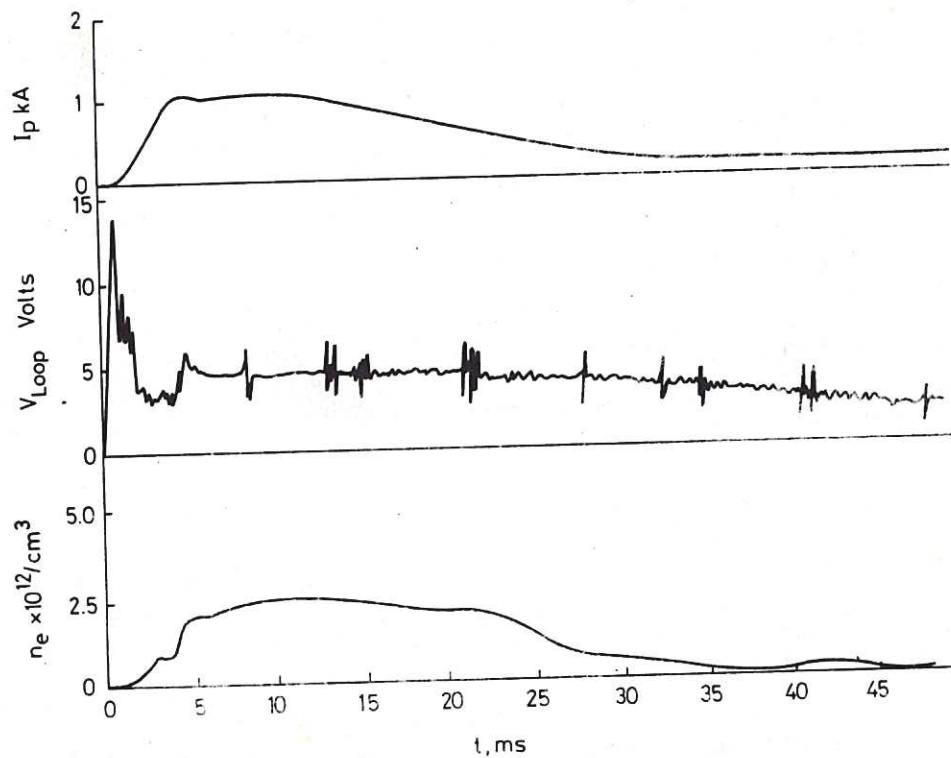


Fig.19(b) Current, voltage and density evolution for a high  $q$  tokamak.



HALQT ( $I_L = 8.5$  kA)

**Fig.20** Current, voltage and density evolution for a helically assisted low q tokamak.



STELLARATOR,  $I_L = 11.8$  kA

**Fig.21** Current, voltage and density waveforms for a stellarator.



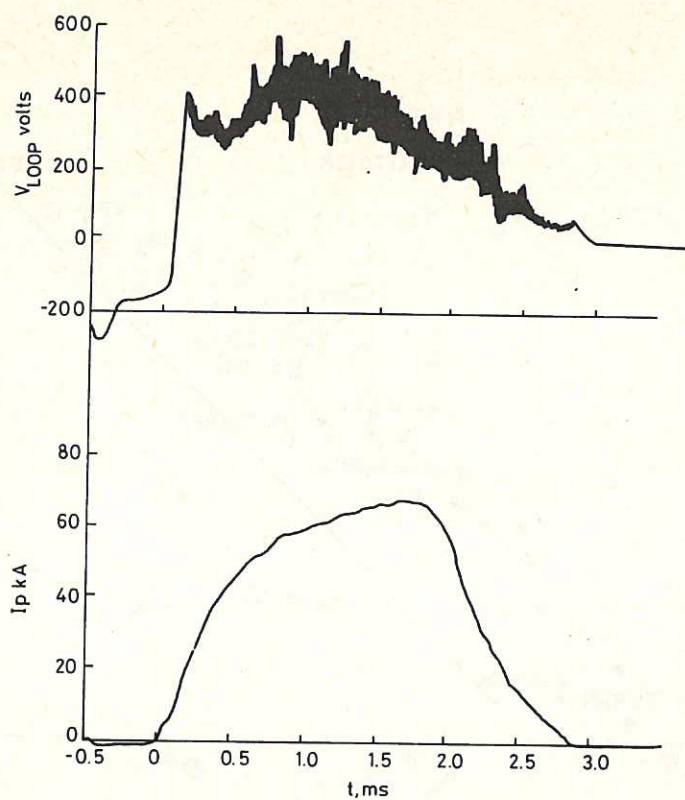


**Fig.22** Current and voltage waveforms for a RFP with an initial toroidal field of 500 G.

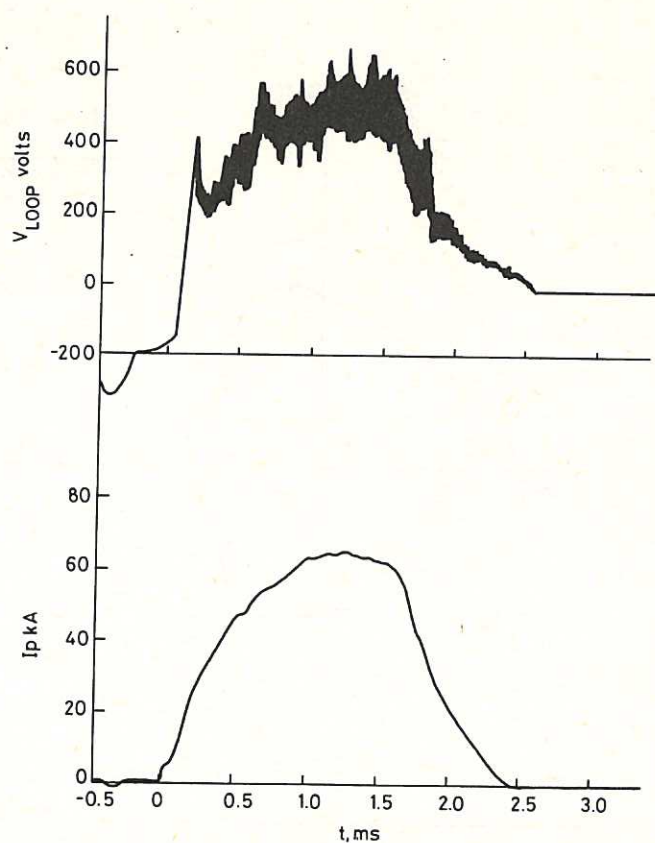


**Fig.23** Current and voltage waveforms for an OHTE with an initial toroidal field of 500 G.

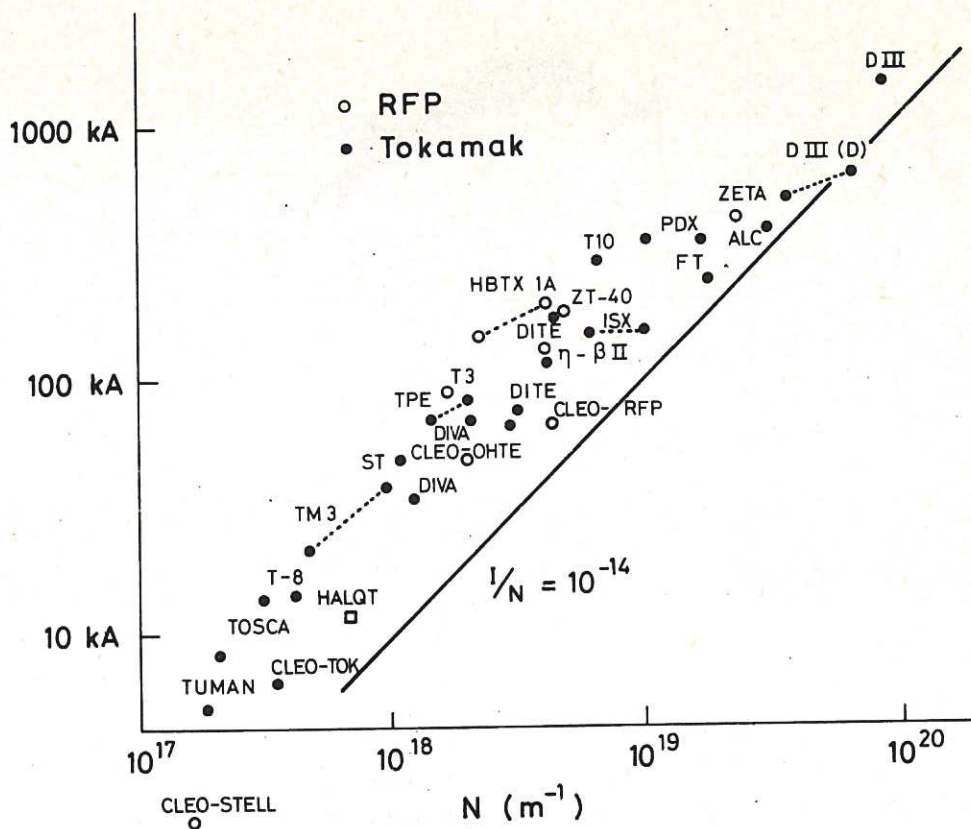


Fig.24 Maximum attainable line density as a function of plasma current for pinches and tokamaks including five points for the different configurations on CLEO.

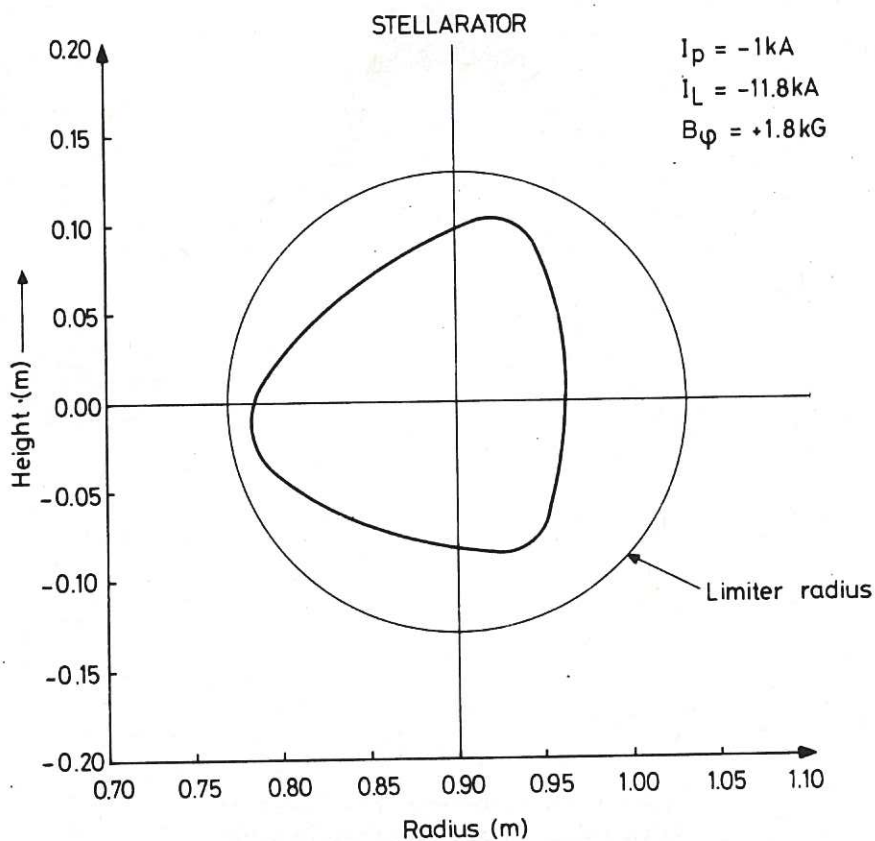


Fig.25 Field line tracing plot of the 'last' closed surface for the stellarator.



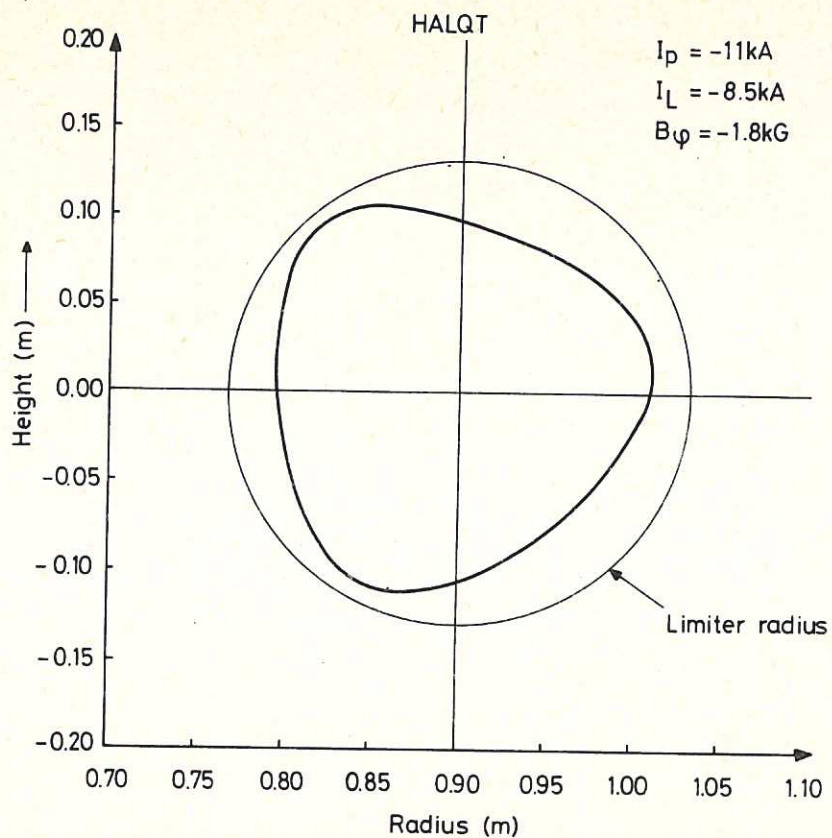


Fig.26 Field line tracing plot of the outer surface for the helically assisted low  $q$  tokamak.

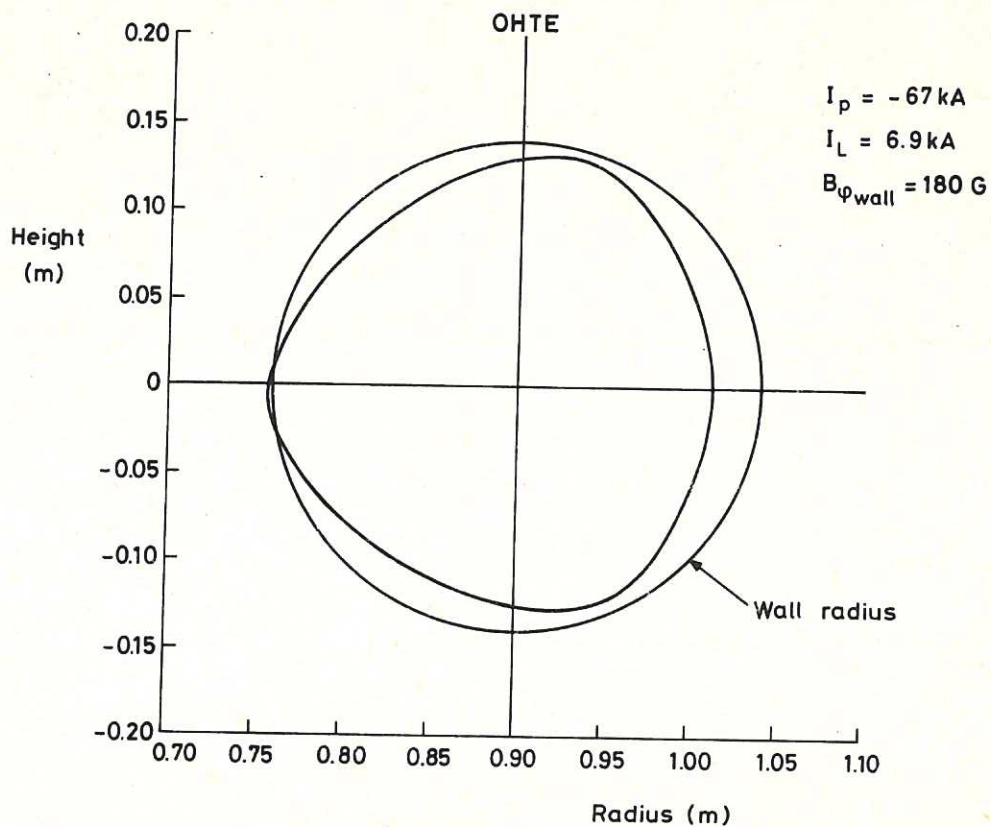
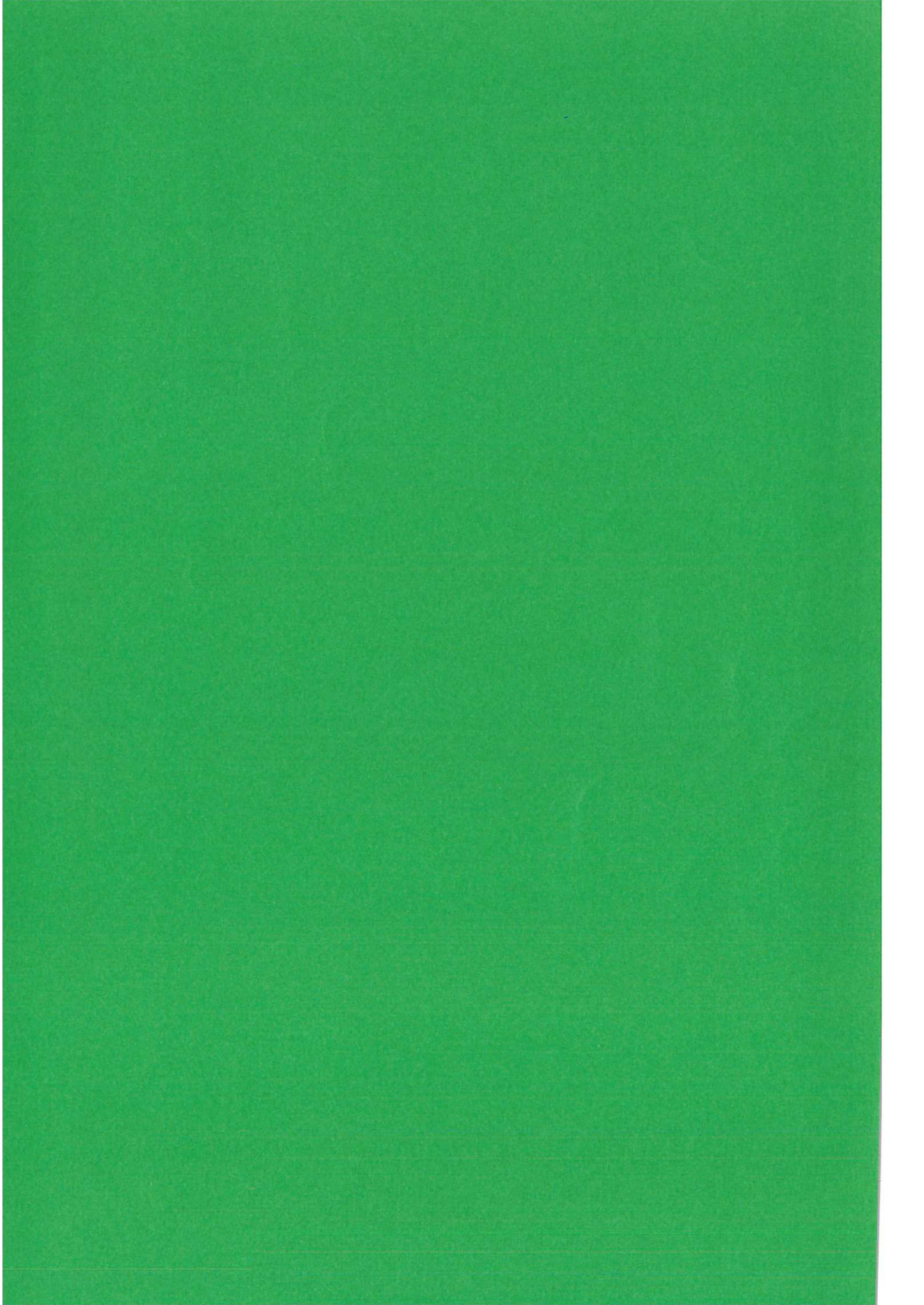


Fig.27 Field line tracing plot of the 'last' closed surface for the OHTE.









HER MAJESTY'S STATIONERY OFFICE

*Government Bookshops*

49 High Holborn, London WC1V 6HB  
13a Castle Street, Edinburgh EH2 3AR  
41 The Hayes, Cardiff CF1 1JW  
Brazennose Street, Manchester M60 8AS  
Wine Street, Bristol BS1 2BQ  
258 Broad Street, Birmingham B1 2HE  
80 Chichester Street, Belfast BT1 4JY

*Government publications are also available  
through booksellers*